Scientia Iranica B (2020) 27(5), 2489–2497

SCIENTIA IRANICA

Sharif University of Technology
**Scientia Iranica**
*Transactions B: Mechanical Engineering*
http://scientiairanica.sharif.edu

*Research Note*

# Deposition of anti-stick coatings to prevent hydrocarbon buildup on truck engines

**M. Awais***

*Department of Industrial Engineering, Taibah University, Medina, Saudi Arabia.*

Received 27 February 2019; received in revised form 21 May 2019; accepted 15 June 2020

**KEYWORDS**
PVD coatings;
Fuel efficiency;
Anti-stick;
Thermal analysis;
Performance ranking.

**Abstract.** The deposition of hydrocarbon buildup on truck engine surfaces may reduce fuel efficiency and the increasing amount of unburned fuel as exhaust gases can lead to environmental hazard. This problematic issue can be resolved by applying anti-stick coatings to engine pistons using Physical Vapor Deposition (PVD) technique. This study investigates a broad range of coating substrate systems including chrome based (CrN, CrAlTiN), oxides (TiOx and ZrOx), carbon based (Graphit-iC$^{TM}$ and Dymon-iC$^{TM}$), and special coating ($TiB_2$) substrate systems to determine their ability to act as anti-stick coatings. All the coatings investigated in this study were applied to polished parts cut from engine piston cylinders. Characterizations were performed after applying droplets of engine oil and heat treating the surfaces up to 400°C. Based on the evaluation of oil adhesion, surface energy, coating thermal stability, surface morphology, and mechanical and crystallographic properties, the anti-stick performance ranking of coatings was suggested for truck engine piston applications in order to improve their performance.



## 1. Introduction

Given the increase in petroleum prices and the pressure of demanding environmental legislations, automobile and truck manufacturers are compelled to produce more fuel-efficient engines. Within the engine, most of the friction-related power losses occur inside the piston-cylinder area, as estimated by Ürgen et al. [1], and ∼15% of total frictional losses occur inside all engine parts. In combustion engines, the explosion of air-fuel mixture in the piston gives engine its power and in general, an engine produces greater power in case more heat is generated. However, an adherent, hard and abrasive carbon (the residual product of air-fuel reaction) layer is deposited on the piston and cylinder surfaces due to burning of oil, which ultimately attenuates the overall performance of the engine (e.g., by increasing friction) [2–5]. Researchers are trying to find the main reasons for this carbon layer, or sometimes called soot buildup, deposited on the automobile engines [2–5]. The variation of engine designs, controlling the gas chamber temperature, and introduction of Exhaust Gas Recirculation (EGR) minimize the release of harmful oxides of nitrogen (NOx) into the environment, but in turn increase the soot buildup on the engine parts [2]. Carbon or soot buildup eventually occurs as a contacting or abrasive layer between two component parts (especially piston and cylinder) and results in abrading the parts due to friction; therefore, oil viscosity increases due to soot buildup and reduces the performance of oil pumps [2].

*. *Tel.: +966 594106269*
*E-mail address: myounas@taibahu.edu.sa*

doi: 10.24200/sci.2020.53021.3014

A possible solution to the build-up of the carbon layer is the deposition of an anti-stick coating on the cylinder surface using the Physical Vapor Deposition (PVD) technique [6–19]. PVD coatings are currently applied to engine components for combating wear and frictional losses mainly. For instance, Bobzin et al. [12] investigated the use of PVD coatings on cylindrical roller thrust bearings and concluded that anti-frication and anti-wear properties of the coatings in the bearing systems improved due to the fine-grained structure of the coatings obtained using PVD techniques. Similarly, Fox-Rabinovich et al. [13] determined that the grain refinement was the major cause of enhanced wear properties of PVD coatings. Navinšek et al. [9] suggested that clean PVD coatings were of better functionality than electroplating and electro-less processes, since the latter cause environmental pollution because of their wastage. In addition, Erdemir and Holmberg [7] and Holmberg et al. [20] found that PVD coatings were characterized by higher cost effectiveness, lower surface roughness, higher hardness, and greater wear resistance than electroplating. McConnell et al. [8] investigated the thermal stability of PVD coatings and found a decreasing trend in wear performance of the coatings with increased temperature conditions. Thus, the main challenge is to develop suitable surface coatings to be able to withstand a higher operating temperature of the engine and higher pressure contact.

Many researchers have investigated PVD coatings such as CrAlTiN and CrN for erosion and corrosion protection [21,22] and they suggested that these multilayered coatings had significant potential to be widely applicable due to their ability to tailor toughness and hardness by modifying the architecture of layer constituents and chemistry. Furthermore, the multi-layered concept was also found beneficial in terms of frictional resistance, as investigated by few more researchers [23,24] when mixing CrN layers with Graphite Like Coatings (GLC) and AlTiN. However, single-layered PVD coatings were found useful as well in terms of wear and corrosion resistance due to better adhesion to the substrates and good crystallinity of such coatings [25–27]. The current work aims to investigate the potential of the most common PVD coatings as an anti-stick layer to avoid buildup of hydrocarbons on engine surfaces such as pistons. The following coating substrate systems are assessed in this study: chrome based (CrN, CrAlTiN), oxides (TiOx and ZrOx), carbon based (Graphit-iC$^{TM}$ and Dymon-iC$^{TM}$), and special coating ($TiB_2$), because these coatings such as CrAlTiN [21,22], CrN [23,24] ZrOx [17], TiOx [25], $TiB_2$ [26], and carbon-based coatings (Graphit-iC$^{TM}$ and Dymon-iC$^{TM}$) have already been investigated by several researchers due to their enhanced anti-wear and anti-corrosion behavior [27]. Carbon- and chromium-based coatings are well known for their applicability to the automotive industry and for their ability to protect engine parts; however, this is the first time that oxide coatings and some special coatings are studied in detail for comparative purposes and, thus, this is the first time that all these significant coatings have been studied collectively for the anti-stick coating applications.

## 2. Materials and methods

A commercial truck engine piston cylinder was obtained and test parts of approximately 1.5 cm × 1 cm × 1 cm in size were cut from the cylinder wall. These parts were then polished using progressively finer grit paper starting at grade 240 and finishing at grade 1200. They were then fine polished with 3 and 1 $\mu$m diamond paste. The polished parts were uncontaminated using methanol first for 5 minutes and then acetone for 5 minutes in ultrasonic bath. Afterwards, ZrOx and TiOx coatings were deposited using a Teer Coating UDP450 system (deposition parameters are provided in Table 1). CrAlTiN, CrN, $TiB_2$, Graphit-iC$^{TM}$, and Dymon-iC$^{TM}$ used in this study were applied to the same substrate by commercial suppliers. All coatings were deposited by magnetron sputtering.

Thermal stability of the coatings is an important criterion for use in truck engines. This was evaluated by heating the coated parts in the air in a box furnace. Samples were heated at 30°C/min up to temperatures of both 300°C and 400°C [28] and were maintained at this temperature for 120 minutes before cooling. The anti-stick properties of the coated parts to carbon buildup were evaluated by applying a drop of heavy-duty engine oil (Castrol GTX Diesel, 15W–40) onto the surface of the coatings. The coated part with oil droplet was then fired in the air in the box furnace. Upon removal from the furnace, the adhesion of the 'burnt oil' was examined using an optical microscope. A scratch was also drawn through the residue using a diamond stylus of a scratch adhesion tester, and the delamination of the burnt oil residue around this scratch using an optical microscope was examined in

**Table 1.** Plasma cleaning and deposition conditions (used for TiOx and ZrOx).

| | **Plasma cleaning** | **Deposition** |
|---|---|---|
| Base pressure (mbar) | $1 \times 10^{-3}$ | $2 \times 10^{-3}$ |
| $O_2$ (%) | – | 67% |
| Target current (amp) | 0.2 | 2 |
| Substrate bias voltage (volts) | 400 | 50 |
| Target-substrate (cm) | 10 | 10 |
| Deposition time (min) | – | 120 |
| Speed of rotation (RPM) | 3 | 3 |

order to provide a qualitative assessment of adhesion of the residue to the surface.

The ball cratering device was utilized in order to determine the coating thicknesses. The spectroscopic ellipsometer measurements (Woollam M2000 variable wavelength ellipsometer) were carried out to verify the measured values. Sessile drop contact angle technique was used in order to measure contact angle and surface energy of the deposited coatings. For this purpose, a video capture apparatus from Dataphysics Instrument (OCA 20) was utilized. Surface free energy was determined using three test liquids: deionized water, ethylene glycol, and diiodomethane. The well-known Owens, Wendt, Rabel and Kaelble (OWRK) method [29] was used to measure polar and dispersive components of surface energies. Philips XRD (X-Ray Diffraction) system with PW 1711 detector and PW 3020 goniometer was utilized to measure crystallinity of the deposited coatings. A normal diffraction mode was used at 40 kV and 40 mA with Cu K$\alpha$ radiation at a scan rate of 1°/min. Wilson Tukon microhardness tester (using 100 gm$_f$ load) was used to measure micro-hardness of the deposited coating substrate systems. Rockwell C indenter with 100 kg$_f$ load was employed to apply an indent to the coating substrate systems which was then assessed using optical microscopy to estimate the adhesion quality of the coatings. This was done by comparing the indentation pattern with the standard scale (HF1: the best adhesion and HF6: the poorest adhesion) [30]. Surface roughness and top surface morphology of the uncoated and coated substrates were investigated by WYKO NT1100 Optical profilometer. An optical microscope was utilized to observe surface morphology, ball crater mark, and Rockwell C indent. The adhesion of the coatings to the substrate was assessed using ST200 scratch adhesion tester (Teer Coatings). In this test, a rockwell diamond tip travels across the coatings at a constant velocity of 10 mm/min and a constant loading rate of 100 N/min, while an increasing normal force is applied to the tested samples. The test was initiated at a starting load (normal force) of 5 N to recognize the start of the scratch track and it was stopped when load reached 50 N. Finally, the critical load $L_c$ was detected at which the first failure in coatings was observed.

## 3. Results and discussion

### *3.1. Characterization of uncoated and coated piston cylinder test samples*

Many pore defects in the piston cylinder substrate material were detected prior to coating. However, the coated surface showed a reduction in the number of pores compared with the uncoated polished surface. The chemical analysis of the uncoated cylinder using Optical Emission Spectroscopy (with a spark source) determined the following elemental compositions: %C = 0.46, %Si = 0.26, %Mn = 0.98, %P = 0.02, %S = 0.03, %Cr = 1.04, %Ni = 0.13, %Mo = 0.21, %Cu = 0.19, %As = >0.39. This analysis result classified the piston cylinder alloy as low alloy steel/medium carbon steel (similar to AISI 4142). These alloys exhibit lower corrosion resistance than high alloy steel such as 316 L. The thickness of the investigated coatings ranged from 0.6 to 2.5 $\mu$m. It should remain clear that while the thickness of the coating is not likely to have a significant effect on the anti-stick properties of the surface, it may however influence coating adhesion to the steel substrates because of internal coating stress [14]; in addition, coating thickness may also influence surface morphology. Optical profilometry was used to monitor surface morphology in this study (Figure 1). From all the coatings examined, TiOx and ZrOx surfaces exhibited the lowest surface roughness ($R_a \approx 5$ nm) and CrN and CrAlTiN the highest ($R_a \approx 15$ nm). Of note, in an earlier study that has evaluated anti-stick properties of DLC (Diamond-like Coating) coated die against aluminum, it was observed that adhesion of the coatings was poor for smoother die surfaces [31].

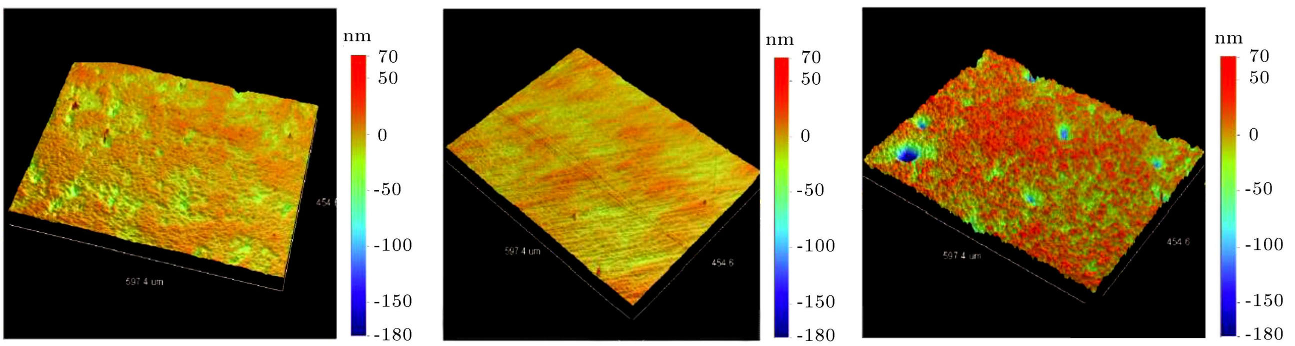


(a) (b) (c)

**Figure 1.** 3D optical profilometry images of the (a) uncoated sample, (b) TiOx, and (c) CrAlTiN-coated polished piston samples.

**Table 2.** Water and oil contact angle/surface energy measurement.

| Coating | Water contact angle (degree) | Polar (mN/m) | Dispersive (mN/m) | Surface energy (mN/m) | Oil contact angle (degree) |
|---|---|---|---|---|---|
| Uncoated | 66 | 9.9 | 32.0 | 42 | 8 |
| CrAlTiN | 94 | 1.5 | 30.2 | 29 | 29 |
| Dymon-iC$^{TM}$ | 91 | 1.5 | 32.4 | 34 | 23 |
| Graphite-iC$^{TM}$ | 87 | 2.5 | 36.7 | 35 | 25 |
| CrN | 84 | 4.0 | 30.0 | 38 | 27 |
| ZrOx | 82 | 4.2 | 29.8 | 31 | 11 |
| $TiB_2$ | 78 | 7.1 | 28.3 | 34 | 25 |
| TiOx | 70 | 8.4 | 33.1 | 41 | 14 |

### *3.2. Evaluation of oil adhesion to uncoated and coated samples*

In order to evaluate the anti-stick properties of the deposited hydrocarbon coatings, contact angle and surface energy were measured on both of the coated and uncoated cylinder parts (Table 2). As shown earlier, coated surfaces exhibited a reduction in surface energy and an associated increase in contact angle, compared to the uncoated piston cylinder sample. Amongst the coatings studied, CrAlTiN and TiOx exhibited the lowest and highest surface energies at 29 mN/m and 41 mN/m, respectively. It was observed that the surface free energy of the coatings was composed of higher dispersion component and lower polar component. The polar component of the surface free energy determines the adhesive characteristic of two opposite surfaces. The uncoated piston cylinder surface displayed the highest polar component (9.8 mN/m) of all coatings (1.5–8.4 mN/m). The variation in contact angle and surface energy for different coatings is influenced by factors such as coating chemistry, structure, surface roughness, etc. It is anticipated that both low polar components with low total surface energy surface are required for anti-stick applications, leading to lower adhesion to opposite surface [29]. From all the coatings tested, CrAlTiN surface exhibited both the lowest surface energy (29 mN/m) and polar component (1.5 mN/m). In order to assess the effect of engine oil adhesion on the coatings, contact angle tests were performed using the Castrol (GTX Diesel oil, 15W–40). As shown in Table 2, an increase in the oil contact angle was identified for the coated sample, compared to uncoated cylinder samples. CrAlTiN and CrN coatings respectively exhibited higher oil contact angles at 29° and 27° than the uncoated steel did at 8°.

To evaluate the adhesion of hydrocarbon residues on the coated piston cylinder parts, tests were carried out by heating the uncoated and coated parts with a drop of engine oil in a box furnace up to temperatures of 400 °C. The adhesion of the oil residue was then assessed by using optical microscopy and the scratch test technique described earlier. Scratch testing was carried out to help differentiate the oil residue adhesion to the test surfaces. The cracking pattern of the oil residue around the scratch formed by the scratch tester is given in Figure 2. This test confirmed that Cr-based coating exhibited the lowest level of adhesion to the oil residue, as shown in Figure 2a. For the Dymon-iC$^{TM}$ coating, a carbon layer was still visible within the scratch track of the coating; in contrast, delamination


(a) (b) (c)

**Figure 2a.** Comparison of oil adhesion on (a) uncoated, (b) CrAlTiN coated, and (c) Dymon-iC$^{TM}$ coated piston samples by the scratch test.

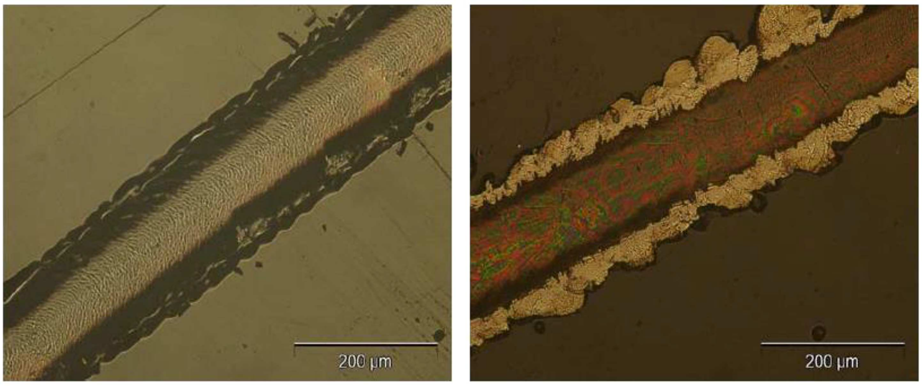


(a) (b)

**Figure 2b.** Comparison of oil adhesion on (a) uncoated and (b) CrAlTiN coated piston samples by the scratch test.

(a) (b) (c) (d)

**Figure 3.** Optical microscopy images of the (a) as-coated CrN coating, (b) thermally treated CrN coating at 400°C, (c) as-coated Dymon-iC$^{TM}$ coating, and (d) thermally treated Dymon-iCTM coating at 400°C.

and spallation of the burned oil layer occurred along the scratch track edge of the CrAlTiN coating (Figure 2b). This may be due to the lower surface energy of the CrAlTiN coating, as detailed earlier.

### *3.3. Thermal stability of the coatings*

To ensure the suitable application of PVD coatings to truck engines, as a precondition, they should exhibit thermal stability up to temperature of 400°C. The morphology of the deposited coatings before and after thermal treatment at both 300 and 400°C was examined using optical microscopy. With the exception of the Dymon-iC$^{TM}$ coating, all the tested coatings exhibited an unchanged surface morphology before and after these heat treatments. The carbon-based Dymon-iC$^{TM}$ coating partially degraded with the heat treatment since significant loss of coating adhesion was observed (Figure 3). The color of the Graphit-iC$^{TM}$ and $TiB_2$ coatings changing after heat treatment may be because of oxidation of the top surface of coatings (confirmed by XRD examination), as suggested by investigators [8,11,18]. The adhesion of the coating-substrate systems before and after heat treatment was measured using the Rockwell-C indentation test. In this test, the Rockwell C indent was compared to the adhesion quality chart, whereas in this chart, HF1 represented good adhesion and HF6 represented total delamination [6, 30]. Table 3 lists the results, and as-coated CrAlTiN, CrN, TiOx, and graphite-IC coatings were measured to have HF1 adhesion. Follow-

**Table 3.** Evaluation of coating adhesion before and after thermal treatment using the rockwell indentation test.

| Coating substrate systems | As coated | Heat treated at 300°C | Heat treated at 400°C |
|---|---|---|---|
| CrN | HF1 | HF2 | HF2 |
| CrAlTiN | HF1 | HF2 | HF2 |
| Graphite-iC$^{TM}$ | HF2 | HF2 | HF3 |
| TiOx | HF1 | HF2 | HF3 |
| Dymon iC$^{TM}$ | HF1 | HF2 | HF3 |
| ZrOx | HF3 | HF3 | HF5 |
| $TiB_2$ | HF3 | HF4 | HF6 |

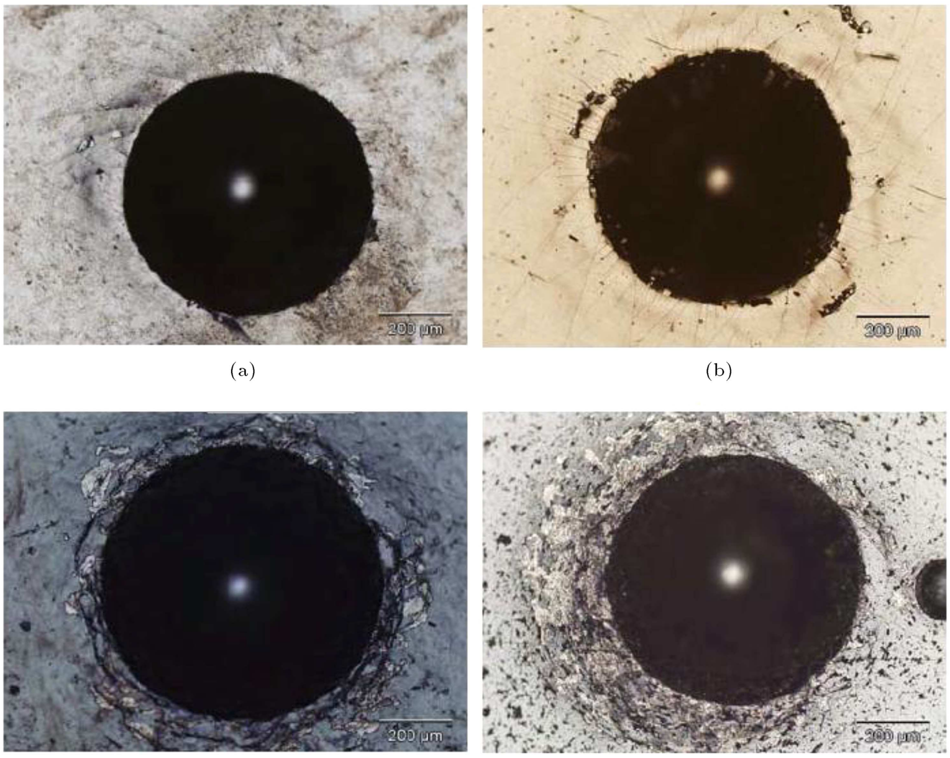

(a) (b) (c) (d)

**Figure 4.** The Rockwell-C indentation spot of the (a) as-received CrN coating, (b) thermally treated CrN coating at 400°C, (c) as-received Dymon-iC$^{TM}$ coating, and (d) thermally treated Dymon-iC$^{TM}$ coating at 400°C for adhesion evaluation.

ing heat treatment, CrAlTiN and CrN coatings were measured to have HF2 adhesion, indicating moderate adhesion. In contrast, even as-coated Dymon-iC$^{TM}$ coatings behaved poorly in terms of adhesion quality; after heat treatment, their performance deteriorated further, resulting in complete delamination of coatings (Figure 4).

Coating adhesion was also assessed using the scratch test technique both before and after heat treatments at 300 and 400°C (Table 4). Both Rockwell and scratch adhesion test results confirmed that Cr-based coatings such as CrAlTiN and CrN exhibited the highest thermal stability and Dymon-iC$^{TM}$, ZrOx and $TiB_2$ showed the lowest thermal stability.

The Vickers micro-hardness of the uncoated and coated piston cylinder samples was carried out before and after thermal treatment to analyze the mechanical stability of the coating-substrate composite system, as shown in Table 5. The two oxide coatings exhibited the same hardness as the substrate. It should be noted that this hardness will be significantly influenced by the bulk hardness of the steel, particularly for these lower thickness ($< 1$ $\mu$m) oxide coatings. In contrast, the hardness values of the Graphite–IC and CrAlTiN coatings were found to be twice that of the uncoated steel. Among the coatings studied in this work, CrAlTiN, $TiB_2$ , CrN, and Dymon-iC$^{TM}$ showed higher composite hardness than other coatings. A reduction of hardness value was observed for all coatings after thermal treatment except for CrAlTiN coating, which exhibited excellent thermal stability in the studied temperature range, as reported previously [32].

An XRD study was carried out in order to identify crystallographic changes in the coating after thermal

**Table 4.** Assessment of coating adhesion using scratch tests before and after thermal treatments.

| Coating conditions | Critical load for failure (N) | | | | | | |
|---|---|---|---|---|---|---|---|
| | **CrN** | **CrAlTiN** | **Graphite-iC$^{TM}$** | **Dymon-iC$^{TM}$** | **TiOx** | **ZrOx** | **$TiB_2$** |
| After coating | 19 | 18 | 29 | 29 | 16 | 2.1 | 11 |
| Heat treated at 300°C | 19 | 17 | 27 | 23 | 11 | 2 | 5 |
| Heat treated at 400°C | 18 | 18 | 25 | 18 | 3 | 2 | 4 |

**Table 5.** Microhardness measurements of coating-substrate composite (error ≈ 2%).

| Coating conditions | Microhardness ($HV_{0.1}$) | | | | | | | |
|---|---|---|---|---|---|---|---|---|
| | Uncoated (steel) | TiOx | ZrOx | CrAlTiN | Graphite-iC$^{TM}$ | CrN | $TiB_2$ | Dymon-iC$^{TM}$ |
| Untreated | 316 | 433 | 403 | 868 | 801 | 1209 | 1221 | 1208 |
| 300 °C | - | 412 | 398 | 800 | 713 | 1181 | 1138 | 1046 |
| 400 °C | - | 334 | 350 | 806 | 553 | 981 | 1059 | 923 |

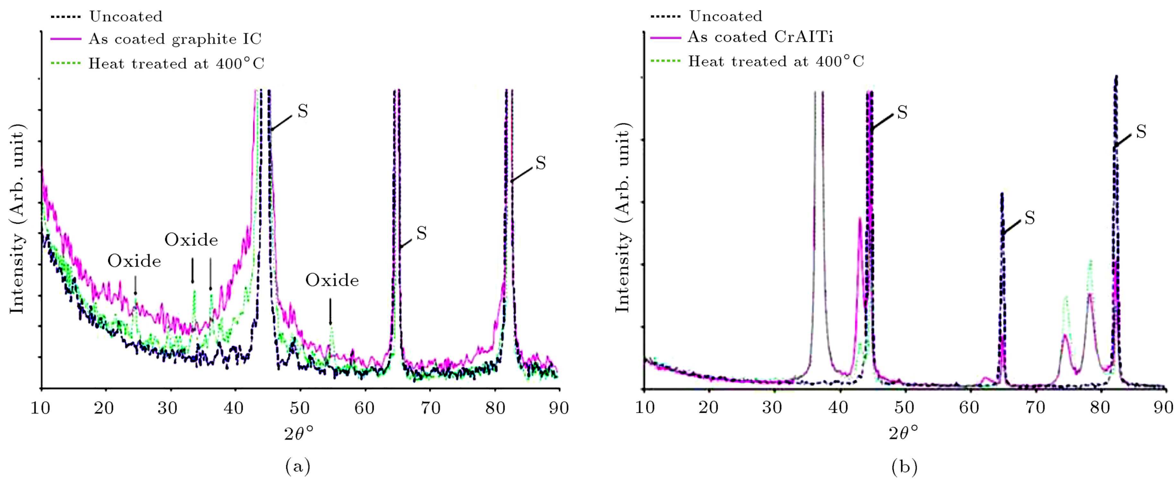


**Figure 5.** The XRD patterns of (a) Graphit-iC$^{TM}$ and (b) CrAlTiN coatings (S = peak from steel work piece) obtained before and after thermal treatment at 400°C.

treatment. No peaks were observed within the XRD spectrum of the as-coated graphit-iC$^{TM}$ coating, indicating the amorphous nature of the film (Figure 5(a)). However, oxide peaks were found in the coating after subjecting it to thermal treatment at 400°C. This indicates the formation of oxides and partial decomposition of coating at a temperature of 400°C [8]. No peaks were observed in the as-coated TiOx sample spectrum, thus demonstrating the amorphous nature of the deposited film. However, after heating to 400°C, a number of diffraction peaks were observed. These peaks were similar to the reference indexed peaks with Powder Diffraction File (PDF) numbers 21–1272, indicating the formation of Anatase phase (TiOx) during the thermal treatment (*vide supra*). In contrast to the results of graphite-IC and TiOx, identical XRD peaks were observed for CrN, CrAlTiN, $TiB_2$ , and ZrOx coatings both before and after thermal treatment. Cr-based coatings mainly consist of the phases of Cr, $Cr_2N$, and CrN before and after thermal treatment. This indicates that CrN and CrAlTiN coatings remain thermally and mechanically stable at 400°C (Figure 5(b)), which is the required temperature for the piston cylinder application [8]. Both $TiB_2$ and ZrOx coatings exhibited structural (phase) stability; however, they showed poor mechanical properties at 400°C, indicating their unsuitability for the piston cylinder application.

## 4. Conclusions

In this study, a range of metal oxides and nitride coatings were deposited on the parts cut from truck engine cylinders. The resulting surface energy of the coatings was lower than that of the uncoated steel. The thermal stability of the deposited coatings was monitored by heating the coated parts in the air up to 400°C. Based on an evaluation of the adhesion of oil and oil residues (after thermal treatment), coating thermal stability, surfaces morphology, and mechanical performance, the following is the hydrocarbon 'anti-stick' ranking allocated to the investigated coatings: CrAlTiN > CrN > TiOx > ZrOx > Graphit-iC$^{TM}$ > $TiB_2$ > Dymon-iC$^{TM}$. It is clear from this assessment that the Cr–based coatings such as CrAlTiN and CrN exhibit the highest anti-stick performance of all the investigated coatings. While this initial study demonstrated the potential of these coatings, it is necessary to further evaluate the effect of coating stoichiometry, thickness, etc. before practical applications.

## Acknowledgments

No funding was provided to carry out this work. However, the author would like to thank Prof. Denis Dowling and Dr. Mahfujur Rahman of Surface Engineering Group, UCD, Ireland for their help and support

to carry out this work. Additionally, a few commercial coatings were examined in this work; however, the author has no conflict of interest in studying these coatings.

## References


1. Ürgen, M., Çakır, A.F., and Erdemir, A. "Advanced tribological coatings for automotive applications", *Intl. Conf. of Tribological Coatings*, Istanbul, Turkey, pp. 1–3 (2004).
2. Abdulqadir, L., Mohd Nor, N., Lewis, R., et al. "Contemporary challenges of soot build-up in IC engine and their tribological implications", *Tribol-Mat. Surf. Interfaces*, **12**(3), pp. 115–129 (2018).
3. Hu, T., Teng, H., Luo, X., et al. "Impact of fuel injection on dilution of engine crankcase oil for turbocharged gasoline direct-injection engines", *SAE Int. J. Engines*, **8**(3), pp. 1107–1116 (2015).
4. Zzeyani, S., Mikou, M., and Naja, J. "Physicochemical characterization of the synthetic lubricating oils degradation under the effect of vehicle engine operation", *Eurasian J. Anal. Chem.*, **13**(4), pp. em34 (1–16) (2018).
5. Wen, Y., Wang, Y., Fu, C., et al. "The impact of injector deposits on spray and particulate emission of advanced gasoline direct injection vehicle", SAE Technical Paper 2016-01-2284 presented at the event of SAE 2016 International Powertrains, Fuels & Lubricants Meeting, https://doi.org/10.4271/2016-01-2284 (2016).
6. Heinke, W., Leyland, A., Matthews, A., et al. "Evaluation of PVD nitride coatings, using impact, scratch and Rockwell-C adhesion tests", *Thin Solid Films*, **270**(1-2), pp. 431–438 (1995).
7. Erdemir, A. and Holmberg, K. "Energy consumption due to friction in motored vehicles and low-friction coatings to reduce it", In *Coating Technology for Vehicle Applications, S.C. Cha, and A. Erdemir*, 1st Edn., pp. 1–23, Springer International, Switzerland (2015).
8. McConnell, M.L., Dowling, D.P., Donnelly, N., et al. "The effect of thermal treatments on the tribological properties of PVD hard coatings", *Surf. Coat. Techn.*, **116**(119), pp. 1133–1137 (1999).
9. Navinšek, B., Panjan, P., and Milošev, I. "PVD coatings as an environmentally clean alternative to electroplating and electroless processes", *Surf. Coat. Techn.*, **116**(119), pp. 476-487 (1999).
10. Lugscheider, E. and Bobzin, K. "The influence on surface free energy of PVD-coatings", *Surf. Coat. Techn.*, **142**(144), pp. 755–760 (2001).
11. Prakash, B., Ftikos, C., and Celis, J.P. "Fretting wear behavior of PVD $TiB_2$ coatings", *Surf. Coat. Techn.*, **154**(2–3), pp. 182–188 (2002).
12. Bobzin, K., Lugscheider, E., Maes, M., et al. "High-performance chromium aluminium nitride PVD coatings on roller bearings", *Surf. Coat. Techn.*, **188**(189), pp. 649–654 (2004).
13. Fox-Rabinovich, G.S., Weatherly, G.C., Dodonov, A.I., et al. "Nano-crystalline filtered arc deposited (FAD) TiAlN PVD coatings for high-speed machining applications", *Surf. Coat. Techn.*, **177**(178), pp. 800–811 (2004).
14. Kano, M. "Diamond-like carbon coating applied to automotive engine components", *Tribol. Online*, **9**(3), pp. 135–142 (2014).
15. Lawal, J., Kiryukhantsev-Korneev, P., Matthews, A., et al. "Mechanical properties and abrasive wear behaviour of Al-based PVD amorphous/nanostructured coatings", *Surf. Coat. Techn.*, **310**, pp. 59–69 (2017).
16. Vetter, J. "Surface treatments for automotive applications", In *Coating Technology for Vehicle Applications*, S.C. Cha, and A. Erdemir, 1st Edn., pp. 91–132, Springer International, Switzerland (2015).
17. Hsu, Y.L., Lee, C.H., Chiu, S.M., et al. "Anti-sticking properties of PVD CrWNx, CrOx and ZrOx coatings on medical electrode application", *Defect Diffus. Forum*, **297**(301), pp. 656–663 (2010).
18. Pellizzari, M. "High temperature wear and friction behaviour of nitrided, PVD-duplex and CVD coated tool steel against 6082 Al alloy", *Wear*, **271**(9-10), pp. 2089–2099 (2011).
19. Silva, F., Martinho, R., and Baptista, A. "Characterization of laboratory and industrial CrN/CrCN/diamond-like carbon coatings", *Thin Solid Films*, **550**, pp. 278–284 (2014).
20. Holmberg, K., Andersson, P., Nylund, N.-O., et al. "Global energy consumption due to friction in trucks and buses", *Tribol. Int.*, **78**, pp. 94–114 (2014).
21. Yang, Q. and McKellar, R. "Nanolayered CrAlTiN and multilayered CrAlTiN–AlTiN coatings for solid particle erosion protection", *Tribol. Int.*, **83**, pp. 12–20 (2015).
22. Huang, W., Zalnezhad, E., Musharavati, F., et al. "Investigation of the tribological and biomechanical properties of CrAlTiN and CrN/NbN coatings on SST 304", *Ceram. Int.*, **43**(11), pp. 7992–8003 (2017).
23. Wang, L. and Nie, X. "Effect of annealing temperature on tribological properties and material transfer phenomena of CrN and CrAlN coatings", *J. Mater. Eng. Perform*, **23**(2), pp. 560–571 (2014).
24. Wan, S., Pu, J., Li, D., et al. "Tribological performance of CrN and CrN/GLC coated components for automotive engine applications", *J. Alloy. Comp.*, **695**, pp. 433–442 (2017).

25. Naghibi, S., Jamshidi, A., Torabi, O., et al. "Application of Taguchi method for characterization of corrosion behavior of TiO2 coating prepared by sol-gel dipping technique", *Int. J. Appl. Ceram. Tec.*, **11**(5), pp. 901–910 (2014).

26. Ranade, A.N., Rama Krishna, L., Li, Z., et al. "Relationship between hardness and fracture toughness in Ti–$TiB_2$ nanocomposite coatings", *Surf. Coat. Techn.*, **213**, pp. 26–32 (2012).

27. Stallard, J. and Teer, D.G. "A study of the tribological behaviour of CrN, Graphit–iC and Dymon–iC coatings under oil lubrication", *Surf. Coat. Techn.*, **188**-189, pp. 525–529 (2004).

28. Schreer, K., Roth, I., Schneider, S., et al. "Analysis of aluminum and steel pistons-comparison of friction, piston temperature, and combustion", *J. Eng. Gas Turb. Power*, **136**(10), 101506 (2014).

29. Owens, D.K. and Wendt, R.C. "Estimation of the surface free energy of polymers", *J. Appl. Polym. Sci.*, **13**(8), pp. 1741–1747 (1969).

30. Jehn, H. and Reiners, G.N.S. (Eds.), *DIN Fachbericht 39, Characterisierung dunner Schichten*, DIN Fachbericht 39, Beuth verlag, Berlin (1993).

31. Fox-Rabinovich, G.S., Weatherly, G.C., Wilkinson, D.S., et al. "The role of chromium in protective alumina scale formation during the oxidation of ternary TiAlCr alloys in air", *Intermetallics*, **12**(2), pp. 165–180 (2004).

32. Bai, L., Zhu, X., Xiao, J., et al. "Study on thermal stability of CrTiAlN coating for dry drilling", *Surf. Coat. Techn.*, **201**(9–11), pp. 5257–5260 (2007).

## Biography

**Muhammad Awais** completed his BSc in Industrial and Manufacturing Engineering from University of Engineering and Technology (UET), Lahore, Pakistan in 2003. He Obtained his MS degree in Mechanical Engineering from Korea Advanced Institute of Science and Technology (KAIST), Daejeon, South Korea (2004–2006) while working in Computer Aided Materials Processing Lab (CAMPLab) on finite element investigations of surface cracking in the hot bar rolling process. He started his PhD in 2008 while working in Surface Engineering group at University College Dublin (UCD), Ireland and completed it in 2011. Dr. Awais has extensive teaching experience obtained from King Abdulaziz University (KAU) and is currently working at Industrial Engineering Department of Taibah University on Manufacturing Processes I and II and CAD/CAM. He has published more than 22 research articles in peer reviewed journals and presented some other in several international conferences and symposiums. His main research interests are especially related to metal oxide coatings, dye-sensitized solar cells, and biomaterials.